Dr. Renée Heilbronner
Handling Topical Editor, Solid Earth

Dear Renée Heilbronner,

Please accept our revised version of the manuscript entitled 'Structural Disorder of Graphite and Implications for Graphite Thermometry' for consideration for publication in Solid Earth. We agree with you that the main message of the manuscript is that the calibrated graphite thermometer is unreliable in deformed rocks, and we hope we have outline this aspect well enough throughout the text. However, we believe it is important to understand why we observe changes in the Raman spectra of graphite after shear deformation, and thus we discuss and interpret the estimated R2 ratios with respect to the parameters of the experiments and our microstructural data. We hope you will agree to retain this discussion.

Nevertheless, we have carefully modified the manuscript in accordance to reviewer`s recommendations and we have implemented the requested changes. We have re-written most of the discussion for better clarity, in particular the parts that interpret (1) shear strain estimates (2) changes in the R2 values and (3) correlation between shear strain and average R2. Also, we agree that the previously suggested shear strain calibration of the graphite thermometer may be inapplicable in natural rocks, and thus we have removed this part from the manuscript. Furthermore, we have added some additional plots showing our mechanical data (included in figure 1), and we also re-calculated the total frictional work per each experiment. Apart from this, we were willing to include the raw mechanical data as well, however the dataset for a single experiment is over a thousand pages, and thus we find it unessential to include. However, we are happy to provide a link to this data to a reader interested in more details.

Below we included the reviewer`s comments and then provided detailed responses to all of them (in red colour). We refer to the revisions of the manuscript with line numbers that are correct with respect to this version of the manuscript with changes accepted.

We hope that the revised manuscript meets the requirements of the high-quality journal Solid Earth, and it will be considered for publication.

Regards,
Martina Kirilova
Corresponding author
Martina.a.kirilova@gmail.com

On behalf of the authors: Virginia Toy, Jeremey S. Rooney, Carolina Giorgetti, Keith C. Gordon, Cristiano Collettini and Toru Takeshita

Comments on se-2017-74-manuscript-version3
"Structural disorder of graphite and implications for graphite thermometry"

The revised version of the manuscript corrects some of the issues, which had been raised by previous reviews by R. Kilian and Oohashi Kiyokazu. However, the main points that had been criticised (interpretation of R2, sample deformation, R2 relation with deformation) and which are essential for the key message of the contribution remain not satisfactorily addressed at all. The authors add additional data or data treatment which, as outlined below does not necessarily help the authors to strengthen their argument against the criticism raised by the reviewers.

In short, the main issues were and still remain to be: 1) increase in R2 needs not to be equivalent to a decreased graphite structural order. 2) The "correction" for shear strain is actually not a correction and the relation of bulk sample strain to deformation which is actually resolved in the slip zones (see below) remains unclear. There are minor issues related to (a) the speculation on deformation mechanisms, (b) the way strain is treated and (c) how the total frictional work was calculated.

The message of the study seems to be that the graphite Raman thermometer is not applicable as-is in deformed rocks. However, the additional interpretations that go into the manuscript (e.g. effect of pressure and sliding velocity, deformation mechanism of graphite in these experiments) are not very well backed by the data and only deflect from the key message.

I recommend that the main issues need to be addressed to make this manuscript a robust publication. The experimental data (at best the raw data, displacement shear-stress, and including sample thickness data) and the Raman data are valuable to provide an insight into the great weaknesses of this Raman thermometry method and to start to understand the influence of deformation on the R2 ratio. However, the partly insufficient data treatment and presentation (e.g. experimental data, bulk strain estimates and sample thinning vs deformation in slip zones, or for example claims on grain sizes and microstructures in the text which are not in accordance with what the figures show) or the speculative interpretation (claims on deformation mechanism and R2 origin) is not what this kind of data has deserved. I am sure the authors could do better, also in cutting short in the speculations and strengthening the analytical parts by more coherent interpretations and a better description of methods for example.

Response: Yes, the key message is that the Raman thermometry is not applicable in deformed rocks, but we think it is very important to understand why and thus we provide additional data. We have clarified our interpretation in accordance with reviewer's recommendation and we hope you will agree to retain this discussion.

1) Origin of reduced R2: The authors claim in numerous passages of the manuscript to report a reduced crystallinity (and it seems they define crystallinity by the presence of intragranular defects, or crystallographic perfection) of graphite. However, what they actually show is a ratio of peaks obtained from Raman spectroscopy (R2). The increase of R2 may be associated with increased intragranular defects or a reduced grain size (as already mentioned in the two previous reviews). It is further claimed that grain size reduction cannot account for the observed change in R2 - a claim the authors do not provide any evidence for. An increase of intergranular lattice defects is pure speculation and actually, newly provided data in the form of TEM images shows the opposite and are not in accordance to what the authors write in the manuscript. While stating that Raman measurements are obtained from within grains (which are said to be >10 µm - where does this number come from, Figure 4b? I'd strongly disagree that any grain size

is evident from this Figure and if so, that 10 µm may be the lower limit), TEM images of the slip surface from where the Raman spectra were obtained show nanometer scale grains. By providing the TEM data, the authors actually contradict what they write in the text, as the data nicely shows that grain boundaries are produced and grain size is largely reduced with grains at the scale of several 10s of nm.

It is nicely demonstrated is that within slip surfaces, R2 is increased and the grain size is very small. What is not shown anywhere is that the increased R2 is related to an increase of intragranular defects - but exactly this is stated throughout the manuscript.

To overcome these ambiguities, providing a definition of crystallinity might be helpful. A crystal may have a low crystallinity because of a high density of (intragranular) lattice defects, however alternatively, an aggregate of "perfect" but extremely small grains may have a low crystallinity since there is a considerable volume which may be influenced by the disorder induced by grain boundaries. The latter definition would go very well with the presented data. Still, with the available data, nothing can be said about the intragranular defect density.

Response: Yes, we agree with this comment and we admit that our discussion needed clarification. Thus, we modified section 4.2 accordingly and we clearly acknowledged the effect of increase in grain boundary density on Raman spectra of graphite. Now, we also use the term ‘aggregate crystallinity’ to avoid any confusion with intragranular crystallinity. (lines 202-212)

2) To correct the graphite thermometer for strain or not: The authors present a fitted function (with surprisingly many digits) for R2 as a function of bulk shear strain or total frictional work. While they correctly note that any sort of strain-related correction will most likely never be feasible in nature (since it is most likely impossible to determine the amount of deformation within a specific graphite aggregate) I do not understand how this fitted function will be a "correction" for the thermometer. Shouldn't a correction provide the "true" R2 after removing the effect of deformation? That's not what the presented functionality provides.

Response: We previously acknowledged that the suggested calibration may be impossible to use in natural rocks. We agree that suggesting a calibration that is perhaps not applicable is pointless, thus we have removed this part from the text.

3) The authors report that most of the strain is accommodated in thin slip surfaces. The variation of apparent bulk shear strain is due to sample thinning (unclear whether extrusion or compaction) so I would not expect this to principally affect the shear surface thickness since they seem to be consist of already highly compacted material. Hence it is pretty surprising to see a relation with the apparent bulk shear strain and R2. Using the mode of R2 instead of the mean, this relation actually becomes not so clear anymore. What is actually the reason to use the mean R2 and not the mode (e.g. by assuming that the most likely result will be analysed) of R2? Even when one would want to assume a relation between bulk strain and strain in slip zones, the chosen measure for strain is at most one of apparent shear strain, and it is not a 1:1 relation with the deformation within the sample. providing shear stress - displacement and displacement - thickness curves may already help with the interpretation of the data.

Response: We understand your concerns about the way we estimated shear strain and we agree that the presented values in fact represent apparent shear strain. Thus, we have included a clarification of this issue in lines 191-193.

We have used average R2 per sample in order to investigate any potential correlation with the overall structural disorder per sample with the conditions of the corresponding experiment. We clearly indicate in the discussion that the correlation between R2 and the estimated shear strain values is a rough approximation (lines 223-225).

4) Calculation of total frictional work: The authors included as an alternative measure to strain the total frictional work, given by the shear stress integrated over the displacement. I cannot reproduce the results presented in Figure 3 or Table 2 using the data of the authors shown in Figure 1a. Also, just by visual inspection, I do not see where the large differences between e.g. experiment 8, 9 and 10 may arise from. Unfortunately for experiments 2, 3, 6,7 no displacement - friction coefficient data was provided. I recommend to double check the calculation procedure for the frictional work and to supply for all experiments displacemnt-shear stress curves. Additionally, it would be beneficial to provide also to provide the displacement-thickness relationships, such that the data could be adequately interpreted.

Response: Thank you for your comment. We checked our calculations of total frictional work and discovered our mistake. The new values are now shown in Table 2. We re-calculated frictional work by using trapezoidal estimation on Matlab, then plotting the resulting data and fitting a power2 function to that.

Below is a snippet from the matlab script that calculates the frictional work:

```
    eval([filename '.FricWorkTrap = trapz(' filename '.ec_disp,' filename
'.Tau);'])
```

Below is a snippet from the plotting of the total frictional work, X and Y are set with the values calculated above:

```
f = fittype('power2');
F = fit(X,Y,f)
txt1 = ['F(x) = ' num2str(F.a) 'x^{' num2str(F.b) '}+' num2str(F.c)];
plot(F,X,Y,'o')
```

We also added the displacement-friction coefficient plots for experiments 2,3,6 and 7 to figure 1a, as well as displacement- thickness plots for all experiments in figure 1c. Plots of displacement vs shear stress do not significantly contribute to the main message, and thus we chose not to include them in the manuscript. But because the reviewer asked for these plots, we provide them in the figure below:

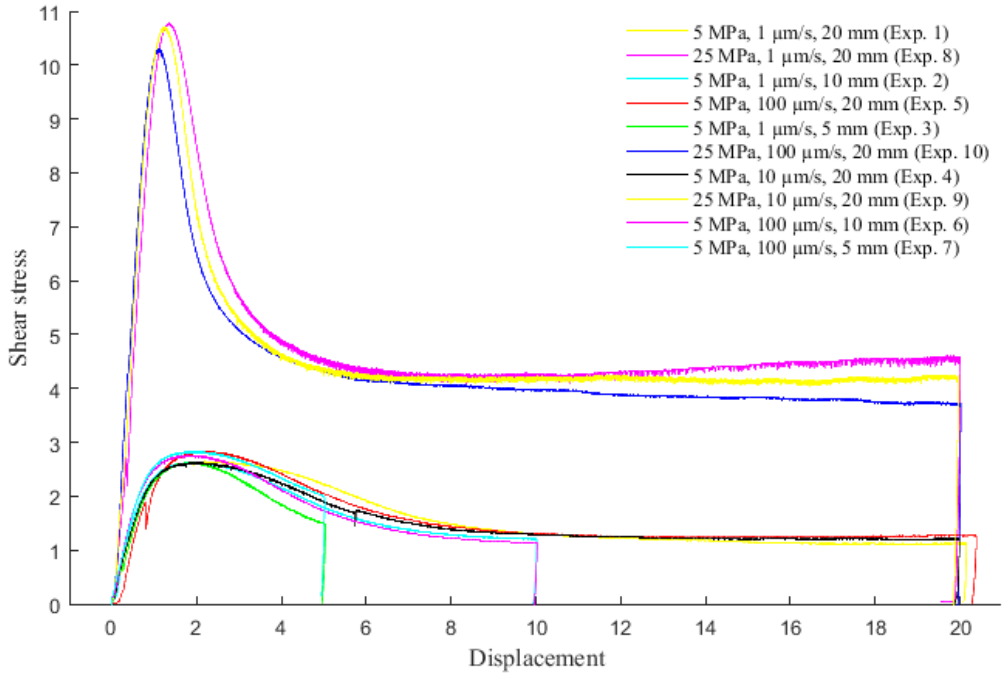

Following some additional comments with reference to the text:

L57: maximum grain size of 160µm : the maximum is in general a very unfortunate measure to say something about a material.

We now present average grain size values (line 57).

L74/75: ".. and summing." summing over?

Replaced with ‘summing up’ (line 75)

I'd also still argue that the measure calculated by the authors is not a shear strain by it's definition in the sense that no strain ellipsoid could be derived from it and it is at best an apparent shear strain. The larger the thinning of the sample, the less related this number is to the deformation of the material. To describe the amount bulk deformation within the material e.g. the aspect ratio of the strain ellipsoid would be more meaningful. However, also for any of these consideration, it needs to be understood whether the sample is loosing volume (is compacting) or extruded somewhere.

Above we agreed that it is apparent shear strain and we have called it that in the text.

Same for Section 3.1.2: While it is stated that the shear strain increase towards higher displacement velocities is basically an artefact of sample thinning (unclear whether extrusion or compaction), this fact is largely neglected in the rest of the ms. However, it not clearly noted that the choosen measure of deformation is with increasing sample thinning increasingly unrelated to the amount of deformation within the sample.

We acknowledged this in the discussion. (lines 195 -198).

L84: Note that the laser spot size is not 1:1 equal with the Raman spot.

Thanks for the comment.

L141/142: "The degree of crystallinity in each sample..." Statement only makes sense when crystallinity would be defined as per aggregate - adding the option that grain boundary density increase decreases the overall crystallinity.

We now talk about R2 instead (line 141).

L147: "..crystallinity varies within each sample see above and speculation, first of all it is R2 which is variable.

We now say '… R2 values vary within a sample…' (line 145)

L151/52: "Furthermore,...." a) table shows R2 not crystallinity as apparently defined by the authors.

Okay, we discuss R2 now (line 149)

b) R2 actually increases (!) with increasing sliding velocities.

Yes, correct. And when R2 increases the crystallinity decreases, which is what we had in the text. The text is now modified, and we talk about increase in R2 instead. (line 149)

L156: work not "force" - also please check calculation procedure.

Thanks for noticing this mistake. We have recalculated frictional work (see comment 4).

L166/167resp. Fig. 4b: grains of 10-50 µm size: unclear if grains or aggregates? Even if these are grains, it does not look like 10 µm is the lower limit. Also compare with the TEM images or Fig. 4d,e. Overall, entire section 3.3.1 does not convincingly demonstrate the large, 10 µm grains within the slip zones.

We now say '…from < 5 to 10 micrometers…' (line 160). TEM data is discussed in the following section 3.3.2.

Section 3.3.2: Figure 5.a if grains are just a few 50-150 nm thick, how would measurements not be covering also grain boundaries. Kinking in graphite (if it is not twinning, but most angles seem larger than the typical twinning relation), Fig. 5b,c requires interlayer slip - and in case this is not crystallographically controlled will result in (001) parallel boundaries, and (001) perpendicular boundaries at kink boundaries, so this is another nice evidence for an increased boundary density beyond the Raman measurement scale. Fig. 5d: I'm not sure what I am seeing but are the authors sure this isn't already beam damaged material?

As we responded to a previous comment, we now acknowledge in the text the effects of increase in grain boundary density on Raman spectra.

L200ff: "...shear strain variation systematically related to the condition of the experiments...shear strain is directly dependent on the applied normal stress". again, the value the authors calculate as shear strain is not a 1:1 measure for the amount of deformation within the material and an artefact of sample thinning.

We removed this part of the discussion.

Section 4.2 Structural disorder of graphite. largely this section should talk about R2 and what was really seen,. e.g. in the TEM images. it is NOT demonstrated that highly crystalline graphite is transformed into disordered graphite with strain!

What can actually be said is that large annealed grains show a low R2 and the deformed material has a (nano)scale grain size, increase of boundaries (grain boundaries, tilt/kink boundaries, ...) and a high R2. It's not possible to say something about crystallinity at the grain scale in the sense of intracrystalline defects.

As we responded to a previous comment, we agree and we have modified section 4.2 accordingly.

L223: "...the results overall validate that structural disorder of graphite can result from shear deformation..." It is close to extremely enigmatic to me how this could be more than a speculation and how the obvious grain boundary area increase is totally ignored.

We now refer to 'graphite aggregates' instead. (line 218).

L229:230: How is it possible to say that no grain boundaries were measured if a) it is not clear where exactly the measurements were undertaken (see question and request from my first review) and b) TEM images of the slip surface show grain boundary spacing at the nm scale and c) the 10 µm grain size remains a speculation (it's totally unclear to me where this number comes from)? Is that some measurement or eyeballing?

We modified this part of the discussion.

L233:30: "...to disorder of the internal structure of graphite rather than grain size reduction." Please see above. This is not consistent with the images you provide!

We modified this part of the discussion.

L241: "...proven..." a) not a proof , b) not shear strain

L249: "We demonstrate that during shearing higher normal stress results in increased shear strain" No. And if layers thin just by compaction (volume reduction) I'd call the latter the reason, not a higher normal stress.

We removed this part from the discussion.

L257:"...effects of shear strain and pressure..." a) if anything at all, the only measure investigated was a bulk apparent shear strain and not pressure but normal stress. Depending on confinement, the pressures my vary of course, but I don't see how to derive/separate a pressure effect from that. Especially since the deformation of graphite seems to happen in very thin slip zones.

We removed this part from the discussion.

L269ff: "...fractured grains...", "brittle processes operated during shearing..resulted in structural disorder of graphite". While fracturing is for example and certainly intimately related to dislocations, it inevitably creates grain boundaries! A more thorough discussion on graphite deformation mechanism might also be more helpful.

Thank you for the comment.

L273: "...would not induce temperatures high enough fro crystal plastic processes" What are those for graphite? And processes such as?

We meant ductile processes. The text is now modified (line 239).

L276: The authors probably mean crystal plastic mechanisms.

Yes, thank you for the comment (line 242)

L277: Plastic deformation? It should be ductile deformation.

Replaced (line 243).

L281: "The crystallographic structure measured by Raman..." No, D1,D2 peaks are measured which could be interpreted in certain ways, e.g. related to structural state of a crystal lattice or e.g. grain boundary density, density of impurities... .

We now say 'The structural order of graphite measured by Raman spectroscopy' (line 251) (Beyssac et al, 2002, 2003).

L285: "...mechanical modification of the graphite structure, which this study has identified..." No, the authors have identified an effect on R2, not directly on the graphite structure.

We rephrased this to '….this thermometer disregards the effects of mechanical modifications on the structure of graphite aggregates, which this study has identified as having a substantial influence on the R2 ratios in deformed graphite gouges at sub-seismic velocities.' (lines 255-257)

L286: " in deformed rocks" misleading, no rocks here beyond a pure graphite gouge.

Replaced with 'deformed graphite gouges' (lines 255-257)

L299: "...we propose a appropriate adjustment based on our dataset" I don't find - beyond my andthe authors doubts on a useful applicability of such an adjustment - any suggestion how this adjustment should look like.

Removed from the text.

L307: "Furthermore, it can be challenging to estimate shear strain in nature ..." Yes it can be challenging and it will be even more challenging to translate bulk rock strain to a deformation seen by a particular grain of graphite within a deformed rock. It should actually also be noted that in the experiments it does seem challenging to estimate the true shear strain/deformation in the bulk: and even more challenging to estimate the deformation in the actually deforming layer of graphite and this is what would be required to start any correction at all.

Removed from the text.

L310: "... graphite crystallinity.." use R2 instead of crystallinity unless properly defined

We modified our conclusions according to the overall revision (lines 272-276)

L312: ""...graphite structural order" see above, use R2

We modified our conclusions according to the overall revision (lines 272-276)

L313: "Microstructural data reveal that this is a result of brittle processes." This needs to be clearly laid out in the results and in the discussion.

It is in lines 235-237.

L314: " trend of increasing shear strain as a function of normal stress and sliding velocity..." this is an effect of sample thinning. And not that this shear strain is does not 1:1 relate to deformation seen by the bulk sample.

Removed from the conclusions.

L318: "...simple shear strain calibration.." a) there is no such thing as "simple shear strain", this is nonsense b) there seems to be substantial thinning of the samples, and while incorrectly treating it as simple shear to calculate an apparent shear strain, the data does not relate to simple shear flow.

Removed from the conclusions.

Rüdiger Kilian

Structural Disorder of Graphite and Implications for Graphite Thermometry

Martina Kirilova[1], Virginia Toy[1], Jeremy S. Rooney[2], Carolina Giorgetti[3], Keith C. Gordon[2], Cristiano Collettini[3], Toru Takeshita[4]

[1] Department of Geology, University of Otago, PO Box 56, Dunedin 9054, New Zealand

[2] Department of Chemistry, University of Otago, PO Box 56, Dunedin 9054, New Zealand

[3] Dipartimento di Scienze della Terra, Università degli Studi La Sapienza, Rome, Italy

[4] Faculty of Science, Earth and Planetary Sciences, Hokkaido University, Sapporo, Japan.

Correspondence to: Martina Kirilova (martina.a.kirilova@gmail.com)

Key Points:

graphite, disorder, thermometry, Raman

Abstract

Graphitization, or the progressive maturation of carbonaceous material, is considered an irreversible process. Thus, the degree of graphite crystallinity, or its structural order, has been calibrated as an indicator of the peak metamorphic temperatures experienced by the host rocks. However, discrepancies between temperatures indicated by graphite crystallinity versus other thermometers have been documented in deformed rocks. To examine the possibility of mechanical modifications of graphite structure and the potential impacts on graphite 'thermometry' we performed laboratory deformation experiments. We sheared highly crystalline graphite powder at normal stresses of 5 and 25 MPa and aseismic velocities of 1 µm/s, 10 µm/s and 100 µm/s. The degree of ~~graphite crystallinity~~structural order both in the starting and resulting materials was analyzed by Raman microspectroscopy. Our results demonstrate ~~consistent decrease of graphite crystallinity with increasing shear strain~~structural disorder of graphite, manifested as changes in the Raman spectra. Microstructural observations show that brittle processes caused the documented ~~structural disorder of graphite~~mechanical modifications of the aggregate graphite crystallinity. We conclude that the calibrated graphite 'thermometer' is ambiguous in active tectonic settings. ~~and we suggest that a calibration that accounts for shear strain is needed.~~

1. Introduction

Organic matter, preserved in sedimentary rocks, can be transformed into crystalline graphite due to structural and compositional changes during diagenesis and metamorphism, a process known as graphitization (Bonijoly et al., 1982; Wopenka and Pasteris, 1993; Beyssac et al., 2002a; Buseck and Beyssac, 2014; etc.). Graphitization is thought to be an irreversible process and graphite is known to remain stable to the highest temperatures of granulite facies and the highest pressures of coesite-eclogite facies (Buseck and Beyssac, 2014). It is generally accepted that the degree of graphite crystallinity, or its structural order, is determined mainly by the maximum temperature conditions experienced by the host rocks, whereas lithostatic pressure and shear strain are considered to have only minor influence on graphitization (Bonijoly et al., 1982; Wopenka and Pasteris, 1993; Bustin et al, 1995). Therefore, graphite crystallinity has been calibrated as an indicator of the peak temperatures reached during progressive metamorphism (Beyssac et al., 2002a; Reitmeijer and McKinnon, 1985). However, in strained rocks discrepancies between temperatures indicated by the crystallinity of graphite vs. other thermometers have been reported (Barzoi, 2015; Nakamura et al., 2015; Kirilova et al., ~~in press~~2017). Thus, numerous authors have speculated that tectonic deformation results in graphite structural modifications that challenge the validity of the existing graphite thermometers (Large et al., 1994; Bustin et al, 1995; Crespo et al., 2006; Barzoi, 2015; Nakamura et al., 2015).

Furthermore, graphite occurrence and enrichment have been documented in several fault zones in the world, e. g. the Alpine Fault zone, New Zealand (Kirilova, et al., ~~in press~~2017), the Hidaka metamorphic belt, Hokkaido, Japan (Nakamura et al., 2015), the Atotsugawa fault system, Japan (Oohashi, et al., 2012), the Tanakura Tectonic Line, Japan (Oohashi et al., 2011), the Err nappe detachment fault, Switzerland (Manatschal, 1999), and the KTB borehole, Germany (Zulauf et al., 1990). In these intensely deformed rocks its presence is of particular interest because its low friction coefficient of $\mu \sim 0.1$ (Morrow et al., 2000) allows graphite to act as a natural solid lubricant (Savage, 1948). The mechanical behavior of graphite has been broadly investigated in both natural and experimental specimens, where it manifests with the lowest μ among sheet structure minerals (Moore and Lockner, 2004; Oohashi et al., 2011, 2013; Rutter, et al., 2013; Kuo et al., 2014, etc.) confirming it could have a significant impact on fault mechanics. It has been experimentally proven that even a small fraction of graphite can have a disproportionally large effect on frictional strength where graphite is concentrated by smearing into interlinked layers (Rutter, et al., 2013).

However, structural changes in crystalline graphite caused by tectonic deformation have not yet been systematically explored. To examine this aspect and to investigate the potential impacts of structural disordering of graphite on the graphite 'thermometer', we have carried out laboratory deformation experiments on highly crystalline graphite powder.

2. Experimental methods

2.1 Sample description

As a starting material in the current study we used synthetic (commercially synthesized) graphitic carbon to avoid complexities arising from variable degree of crystallinity in natural carbon materials. Initially, the material was crushed to ~~maximum~~ average grain size of 100~~160~~ μm in a RockLabs Swing (TEMA) mill. The resulting fine graphitic powder was annealed at 700˚C for two hours in a Lindberg Blue M Muffle Furnace to achieve full graphitization, which is known to occur at this temperature in the absence of other variations in physical conditions (Buseck and Beyssac, 2014). This was used as the starting material for the deformation experiments.

2.2 Experimental procedure

In total, 10 deformation experiments were performed at room temperature and room humidity in the Brittle Rock deformAtion Versatile Apparatus BRAVA (Collettini et al., 2014), at INGV, Rome. For each experiment two 3-mm thick layers of synthetic graphite gouges were placed in between three grooved forcing blocks in a double-direct shear configuration (e.g. Dieterich, 1972). The two side blocks are held stationary, and the central forcing block is driven downward causing shear to occur within the graphite gouge layers. Normal stress is applied by the horizontal piston in load-feedback control mode and shear displacement accomplished by the vertical piston in displacement-feedback control mode. Forces are measured with stainless steel load cells (± 0.03 kN) and displacements are measured with LVDTs (± 0.1 μm) attached to each piston. Experiments have been conducted at normal stresses of 5 MPa or 25 MPa and aseismic sliding velocities of 1 μm/s, 10 μm/s and 100 μm/s. The experiments were carried out to total displacements of 20 mm. In addition, some experiments were stopped at 5 mm and 10 mm and the specimens were then recovered to reveal graphite structural changes that took place during different amounts of total deformation. The coefficient of friction (μ) was calculated as the ratio of measured shear load to measured normal load ($\mu = \tau / \sigma_n$, where τ is shear stress and σ_n is effective normal stress). The average shear strain within the layer was calculated by dividing shear displacement increments by the measured layer thickness and summing up. The displacement values of the vertical and horizontal load points were corrected for the elastic stretch of each load frame, taking into account that the machine stiffness is 1283 kN/mm on the horizontal axis and 928.5 kN/mm on the vertical axis. In addition, we calculated total frictional work for each experiment as a function of shear stress integrated over the total displacement (Beeler, 2007).

2.3 Raman microspectroscopy

~~The degree of graphite crystallinity~~Raman spectra of graphite was measured by an Alpha 300R+ confocal Raman microscope (WITec, Ulm, Germany) with a 532 nm laser (Coherent, Santa Clara, California), located at the Department of

Chemistry, University of Otago, New Zealand. The laser (3.0 mW) was focused on the samples with a 50× Zeiss objective. The scattered light was dispersed with a 1200 g/mm grating. The combination of the 50× objective and 532 nm laser wavelength produced a laser spot size of approximately 412 nm in diameter. The integration time of each spectrum was 2 seconds with 50 co-additions (100 seconds in total). The spectra were calibrated using the Raman band from a silicon wafer prior to each set of measurements.

The collected spectra were pre-processed in GRAMS AI 9.1 (Thermo Fisher Scientific Inc.), where cosmic spikes were removed, and a multi-point linear baseline offset was performed. This was followed by peak fitting three Lorentzian-Gaussian functions to each spectrum with a linear baseline over 1000 - 1700 cm^{-1}. For each spectrum, the area ratio was calculated ($R2 = A_{D1} / (A_G + A_{D1} + A_{D2})$, where A*i* is the area of the *i*th peak, G band is the main high frequency band of graphite, D1 and D2 bands are defect bands observed in the first order Raman spectrum of graphite) (Wopenka and Pasteris, 1993; Beyssac et al.., 2002a).

2.4 Scanning electron microscopy

Microstructural analyses of the graphite gouge recovered from the biaxial apparatus were carried out using a scanning electron microscope (SEM). Some SEM images were acquired from the shiny surfaces of the graphite layers that had been parallel to the center and or side forcing blocks (Y-Z sections), with a Zeiss Sigma field emission scanning electron microscope (VP FEG SEM) at the Otago Centre for Electron Microscopy (OCEM), University of Otago, New Zealand. The instrument was operated in variable pressure mode (VP) at 15 kV using a working distance (WD) of 7 – 8 mm and a VPSE (VP-mode secondary electrons) detector. In addition, polished thin sections cut perpendicular to the surface of contact with the center and side forcing blocks (X-Z sections) were imaged on a JEOL JSM-6510 SEM at the University of Potsdam, Germany, where high-resolution secondary electron images were collected at 20 kV and a WD of 10 mm.

2.5 Transmission electron microscopy

Transmission electron microscopy (TEM) was used for detailed microstructural characterization of the shiny surfaces. High-resolution TEM images were collected by using a JEM-2010 electron microscope, located at the University of Hokkaido, Sapporo, Japan. The instrument was operated at 200 kV with LaB6 filament. TEM foils (with size of 12 x 5 µm and thickness of 1 µm) milled by FIB perpendicular to the shiny surface (X-Z section) were placed on a carbon coated film, and examined by using dual-axis tilting holder.

3. Results

3.1 Mechanical data

Our experiments allowed us to investigate graphite mechanical behavior and structural modifications under various sliding velocities, normal stresses and shear strain. These conditions are summarized in Table 1. The estimated total frictional work for each experiment is shown in Table 2.

3.1.1 Friction variations

Over several mm of displacement, the friction coefficient shows a similar evolution trend in all experiments. On a plot of friction coefficient vs. displacement (Fig. 1a), the friction coefficient (μ) delineates a curve characterized by a rapid increase to an initial peak friction coefficient (μ_{peak}), followed by a subsequent exponential decay towards a steady-state friction coefficient (μ_{ss}) over a slip weakening distance. The shapes of the friction-displacement curves vary with the normal stress applied and are steeper for the experiments conducted at 25 MPa than the ones at 5 MPa (Fig. 1a) i.e. the displacement required to achieve steady-state decreases at higher normal stress. In addition, the values of both μ_{peak} and μ_{ss} (Fig. 1a; Table 1) are significantly lower in the experiments at 25 MPa (μ_{peak} = ~0.4; μ_{ss} = ~ 0.1) than in the experiments at 5 MPa (μ_{peak} = ~0.5; μ_{ss} = ~ 0.2) (where μ_{ss} values were read at the end of each experiment). Plots of μ at all sliding velocities (Fig. 1a) show subtle variations in μ_{peak} and μ_{ss} with change of the applied sliding velocities (Fig. 1a; Table 1).

3.1.2 Shear strain variations

Plots of friction coefficient vs. shear strain (Fig. 1b) show significant variations in shear strain attained over equivalent sliding displacements. The estimated shear strain values are a geometric consequence of different thickness changes, which are visualized on plots of layer thickness vs. displacement (Fig. 1c). Consideration of the shear strain at equivalent sliding velocities but different normal stresses demonstrates that shear strains achieved during the 5 MPa experiments are approximately half of those at 25 MPa (Fig. 1b; Table 1). In addition, the experiments at 25 MPa demonstrate a dramatic increase in shear strain with increasing slip velocity (Fig. 1b; Table 1), whereas at low normal stress we do not observe any systematic variations associated with changes in sliding velocities (Fig. 1b, c and d). ~~Fig. 1c and d show the experiments at low shear strain used to characterize graphite structural changes in the early stages of deformation (Table 1).~~

3.2 ~~Graphite crystallinity~~Raman spectra of graphite

All the experiments resulted in the development of shiny smooth surfaces with gentle slickenlines (macroscopic fine grooves, parallel to the slip direction as defined by Toy et al., ~~in press~~2017). Raman spectra obtained on the top of these

surfaces, that had accommodated most of the induced deformation, are compared to Raman spectra from the starting material ~~to identify the effects of mechanical deformation on graphite crystallinity.~~ .

Raman data from 20 spectra per sample are presented in Supplementary material 1~~1~~ (~~S1~~S1). Representative spectra for each sample are illustrated in Fig. 2, which shows spectra displaying the least (left column) and the most (right column) disordered graphite within a sample (i.e. lowest and highest R2 values respectively). Spectra that were typical of the average for each sample are also presented (middle column). Experiments 3 and 7 were stopped at only 5 mm displacement and resulted in extremely fragile deformed surfaces, which were unable to be extracted without them breaking into pieces too small to obtain spectra from. Thus, ~~graphite crystallinity~~Raman spectra was not measured in these experiments.

All the acquired spectra show typical G, D1 and D2 bands, respectively at ~1580 cm^{-1}, ~1350 cm^{-1} and ~1620 cm^{-1} (~~S1~~S1). ~~The degree of graphite crystallinity in each sample could thus be calculated by using~~ Thus, we could calculate the area ratio R2 for each spectrum (Fig. 2; ~~S1~~S1). Raman spectra collected from the starting material show R2 values ranging from 0 to 0.327 (Fig. 2)~~, corresponding respectively to fully crystalline and highly organized graphite~~. Spectra acquired from the deformed surfaces show higher R2 values ~~–~~(Fig. 2; ~~S1~~S1). The most ~~crystalline~~ ordered graphite with R2=0.330 was collected in Exp. 2 (Fig. 2) while the most disordered graphite with R2=0.661 resulted from Exp. 10 (Fig. 2).

As ~~graphite crystallinity~~ R2 values var~~ies~~y within a sample (Fig. 2; ~~S1~~S1), we examine average R2 values for each one and compare them with applied normal stress, sliding velocity, shear strain, and total frictional work (Table 2). The starting material has average $R2_{pre\text{-}shear\ graphite}$ = 0.173, whereas all deformed samples have higher average R2 values (Table 2). Analyzing the average R2 values for deformed samples reveals that graphite is more disordered in the high normal stress experiments (Table 2) than in the experiments at 5 MPa. Furthermore, in the experiments at 25 MPa the average ~~graphite crystallinity~~R2 ~~decreases~~ increases with increasing sliding velocities (Table 2). In contrast, at low normal stress, we do not observe any dependence of the degree of graphite ~~crystallinity~~ structural order on the applied sliding velocities (Table 2). Overall graphite appears as most disordered in the experiments where the highest shear strain was achieved (Table 2). The relationship between average R2 and shear strain is illustrated in Fig. 3a by fitting a power function with a correlation coefficient R^2 = 0.95. Fitting a power function to average R2 and total frictional ~~force~~ work did not show~~ed~~ a consistent correlation (Fig. 3b). The experiments 2 and 6 at low normal stress, which were stopped at 10 mm displacement and accommodated the least amount of shear strain, contain the least disordered graphite (Fig. 3; Table 2).

3.3 Microstructural characteristics

3.3.1 Scanning electron microscopy (SEM)

Similar microstructural features were observed in all the deformed samples. SEM images obtained from the sample deformed during experiment 8 are presented to demonstrate our observations (Fig. 4).

These high-resolution images in Y-Z sections reveal that the shiny surfaces are decorated by closely spaced (from < 5 to 10 micrometers) slickenlines (Fig. 4a), on top of a smooth continuous layer. In places, the continuity of this layer is interrupted by fine (~1 to 2 micrometers in width) fractures (Fig. 4a), with random orientation compared to the slip direction. Occasionally, the deformed surface appears as completely disrupted, and is decorated with small~~er~~ graphite grains (from 50 to <10 ~~to 50~~ micrometers in size), oriented nearly parallel to the shear direction (Fig. 4b). In X-Z sections this highly deformed surface is observed as a thin slip-localized zone, composed of well-compacted layer of aligned graphite grains (Fig. 4c). This localized shear surface is underlain by a zone of randomly oriented, inequigranular, irregular graphite grains (Fig. 4d). In places, most of the graphite grains are aligned with their basal (001) planes parallel to the slip direction, and form compacted layers, defining a weakly-developed fabric (Fig. 4e). There has been some dilation along these cleavage planes, and the spaces thus created are filled with smaller graphite grains with their (001) planes sub-perpendicular to the shear direction (Fig. 4e). Locally, intensely fractured grains are also observed (Fig. 4f).

3.3.2 Transmission electron microscopy (TEM)

TEM was used to examine the microstructure of the material that makes up the shiny surfaces (Fig. 4c). TEM analyses were performed on foils cut perpendicular to this surface. Fig. 5 shows characteristic TEM images obtained from the sample recovered from experiment 8.

Graphite grains in this well-compacted layer have basal planes predominantly aligned with the shear plane, as were observed in SEM images. However, adjacent grains show slightly different orientations (Fig. 5a). In addition, kink folded graphite grains are observed in multiple locations in the foils (Fig. 5b, c), which yields a ‘wavy layering’ at a small angle to the shear direction (Fig. 5b). In isolated areas, there are also some smaller grain fragments with random orientation (Fig. 5d).

4. Discussion

4.1 Mechanical behavior

Graphite in our experiments shows mechanical behavior consistent with other mechanical studies of pure graphite gouges. Our results display low μ_{ss} values (from ~0.1 to ~0.2; Table 1) as did the low-pressure deformation experiments of

carbonaceous material performed by Morrow et al. (2000), Moore and Lockner (2004), Oohashi et al. (2011, 2013), Kuo et al. (2014), and Rutter et al. (2013). The low frictional strength of graphite is well known and has been attributed to its sheet structure composed of covalently bonded carbon atoms held together only by van der Waals forces. These weak interlayer bonds along (001) planes are easily broken during shear (Moore and Lockner, 2004; Rutter, et al., 2013). Initial μ_{peak} followed by strain weakening during deformation experiments of graphite gouges has been previously explained with the work involved in rotating the grains with their (001) planes sub-parallel to the shear surfaces, which puts them in the optimal position for shearing along the weak interlayer bonds (Morrow et al., 2000; Moore and Lockner, 2004; Rutter, et al., 2013).

~~Controversially, Oohashi et al. (2011) reported an absence of μ_{peak} in pure graphite gouges sheared at $\leq$ 2 MPa with sliding velocities of 1.3 m/s. Instead shearing started and continued at a similar μ throughout their experiments. We hypothesize that higher velocities result in more efficient reorientation of graphite grains, and therefore, μ_{peak} is not present in experiments carried out at seismic rates. We also acknowledge that the imposed velocities in the experiments by Oohashi et al. (2011) were substantially different to ours, and shearing at those seismic rates may cause frictional heating. Therefore, graphite frictional strength in their experiments may be related to thermally activated weakening mechanisms (Di Toro et al., 2011) that are only significant at these high velocities.~~

Plots of layer thickness vs. displacement (Fig. 1c) show that the initial compaction resulted in layers with different thickness prior to shearing. Therefore, we refer to the estimated shear strains (or the ratio of shear displacement to measured layer thickness) as apparent shear strains. Correlation between these values and the conditions of the experiments show that the apparent shear strains are significantly higher in the experiments performed at 25 MPa than the ones at 5 MPa mainly due to better compaction of the sheared graphite gouges (Fig. 1c). The apparent shear strains increase with increase in the applied sliding velocities in the high normal stress experiments (Fig. 1b), however this trend also reflects differences in the layer thickness prior to shearing (Fig. 1c). The latter interpretation is also supported by the absence of similar correlation during the low normal stress experiments. Nevertheless, there are too few of these relationships to fully characterize the effect of normal stress and sliding velocity on shear strain accumulation in graphite gouges, and more mechanical data of this sort need to be collected in future.

~~We also observed shear strain variations in the various samples (Fig. 1b, c and d) that are systematically related to the conditions of the experiments. The calculated shear strain (or the ratio of shear displacement to measured layer thickness) is directly dependent on the applied normal stress, and shear strains are significantly higher in the experiments performed at 25 MPa than the ones at 5 MPa due to better compaction and thinning of the sheared graphite gouges. Furthermore, sliding velocities also play a role in the accommodated total shear strain, and shear strain increases with increase in the applied sliding velocities but only in the high normal stress experiments (Fig. 1b). As we previously suggested, higher velocities may result in more efficient reorganization of graphite grains, and thus further progressive thinning of the graphite gouges~

~~occurred. However, we cannot explain the absence of similar trend at the 5 MPa experiments by our results. There are too few of these relationships to fully characterize the effect of sliding velocity on shear strain accumulation in graphite gouges, and more mechanical data of this sort need to be collected in future.~~

4.2 Structural disorder of graphite

~~Our experimental study clearly demonstrates transformation of fully/highly crystalline graphite (with R2 ratios ranging from 0 to 0.327; Fig. 2; S1) into comparatively poorly organized graphitic carbon (with R2 ratios up to 0.661; Fig. 2; S1), which indicates significant graphite disorder with increasing strain and total frictional work at the tested aseismic sliding velocities (Fig. 3). The estimated bulk shear strains (Table 1) are likely to be significantly lower than the shear strains accommodated within the thin shear surfaces. However, we expect the strain variations within these surfaces to be directly related to the measured bulk shear strains. Nevertheless, we refer to the above relationship as a rough approximation. We also acknowledge that the slickenlined surfaces that were produced experimentally contain some graphite that yield spectra comparable to those acquired from the starting material i.e. there is highly crystalline graphite that appears as unaffected by the deformation. However, at least some of these spectra are derived from undeformed graphite powder that underlies the shear surfaces and could not be entirely removed during sample preparation due to the fragile nature of the samples. It is also possible that some non-deformed graphite powder was accidently measured through the fractures that are cross-cutting the accumulated shear surfaces (Fig. 4a). But even if some graphite did not undergo mechanical modification during the experiments, the results overall validate that structural disorder of graphite can result from shear deformation subsequent to the graphitization process.~~

~~We evaluate the documented disorder of the crystal structure of graphite by analyzing variations in R2 ratios, which depend on the increase of defect bands (D1 and D2) in the Raman spectrum of graphite. This relationship is a well known crystallinity index of graphite that shows the degree of maturity of the carbonaceous material (Wopenka and Pasteris, 1993; Beyssac et al., 2002a; etc.). Alternatively, it may reflect increase in the grain boundary density (Tunistra and Koening, 1970; Pimenta et al., 2007). However, we aimed to avoid grain boundaries during spectra acquisition, which was possible due to the laser spot size of 412 nm, which is much smaller than the graphite grains in our samples (>10 microns, Fig. 4b). We acknowledge that some of the spectra may have been accidentally obtained in close proximity to grain boundaries, however occasional measurements of this sort are unlikely to affect the average R2 per sample. Thus, we attribute the detected increase in D bands in our experimental data to disorder of the internal structure of graphite rather than grain size reduction.~~ We evaluate the structural order of graphite by analyzing variations in R2 ratios, which depend on the increase of defect bands (D1 and D2) in the Raman spectrum of graphite. Previous studies have documented increases in R2 with decreasing degree of graphite crystallinity (Wopenka and Pasteris, 1993; Beyssac et al., 2002a, b). Therefore, our experimental study may demonstrate transformation of fully/highly crystalline graphite (with R2 ratios ranging from 0 to 0.327; Fig. 2; S1) into

comparatively poorly organized graphitic carbon (with R2 ratios up to 0.661; Fig. 2; S1). However, we do not have direct evidence suggesting intragranular deformation. Alternatively, the observed increase of defect bands is also likely to reflect increase in the grain boundary density (Tunistra and Koening, 1970; Pimenta et al., 2007). The latter is further supported by our microstructural data that reveals the existence of fine graphite grains (ranging from 50 µm to nm scale grains; Fig. 4, 5) which are significantly smaller in size than the average grain size of the starting material (100 µm). We interpret that shear deformation caused intense grain size reduction, and hence increase in the grain boundary density, that was reflected in the Raman spectra as a decrease of the overall aggregate crystallinity.

~~Our findings contradict the paradigm that the degree of graphite crystallinity is determined by an irreversible maturation of carbonaceous material (Bonijoly et al., 1982; Wopenka and Pasteris, 1993; Beyssac et al., 2002a; Buseck and Beyssac, 2014). Therefore, graphite should not be considered as a stable mineral (Buseck and Beyssac, 2014), especially in active tectonic settings, where mechanical motions, such as fault creep, may cause disordering of the structure of carbonaceous material that formed during typical graphitization processes. Similar assumptions have been made on graphite in intensely deformed cataclasites (comprising crushed mylonitic chips floating in a fine-grained matrix) that is significantly disordered in comparison with graphite in the spatially associated mylonitic rocks (Kirilova et al, in press; Nakamura et al., 2015).~~

We also acknowledge that the slickenlined surfaces that were produced experimentally contain some graphite that yield spectra comparable to those acquired from the starting material i.e. there is highly ordered graphite that appears as unaffected by the deformation. However, at least some of these spectra are derived from undeformed graphite powder that underlies the shear surfaces and could not be entirely removed during sample preparation due to the fragile nature of the samples. It is also possible that some non-deformed graphite powder was accidently measured through the fractures that are cross-cutting the accumulated shear surfaces (Fig. 4a). But even if some graphite did not undergo mechanical modification during the experiments, the results overall validate that structural disorder of graphite aggregates can result from shear deformation subsequent to the graphitization process.

To understand the potential causes for the documented structural disorder of graphite, we compared the measured average R2 with the parameters of the performed experiments. Our data show a good correlation between the average R2 and the apparent shear strain at the tested aseismic sliding velocities (Fig. 3). However, these bulk shear strains (Table 1) are likely to be significantly lower than the shear strains accommodated within the thin shear surface and thus, we refer to the above relationship as a rough approximation. Nevertheless, previous authors have also suspected that shear strain may play an important role for graphite modifications, and evidence for this has been found in graphite crystallinity variations in natural samples from active fault zones (Kirilova et al, 2017; Nakamura et al., 2015), and strained rocks in metamorphic terrains (Barzoi, 2015; Large et al., 1994). Thus, we speculate that shear strain may play an important role for the final structural

order of graphite aggregates and consequently, the previously proposed model of progressive graphitization due to increase of temperature (Bonijoly et al., 1982) does not completely reflect the graphite formation mechanisms.

~~We have experimentally proven that shear strain can not only affect the final structural order of graphite but also manifests as a controlling parameter in the transformation process (Fig. 3a; Table 2). Previous authors have suspected that shear strain may play an important role for graphite modifications, and evidence for this has been found in graphite crystallinity variations in natural samples from active fault zones (Kirilova et al, in press; Nakamura et al., 2015), and strained rocks in metamorphic terrains (Barzoi, 2015; Large et al., 1994). Thus, we conclude that the previously proposed model of progressive graphitization due to increase of temperature (Bonijoly et al., 1982) does not completely reflect the graphite formation mechanisms.~~

~~Furthermore, graphite can form or be transported at various depths by tectonic processes, and therefore, it can be exposed to different lithostatic pressures, and hence different normal stresses. We demonstrated that during shearing higher normal stress results in an increase of shear strain (Fig. 1b), and thus causes a higher degree of graphite disorder (Fig. 3a; Table 2). This outlines the significant effect of lithostatic pressure on graphite crystallinity that has been undervalued until now (Bonijoly et al., 1982; Wopenka and Pasteris, 1993; Bustin et al, 1995; Beyssac et al. 2002b). Previous experimental studies have identified initiation and enhancement of graphitization under pressure (i. e. increase in graphite crystallinity) but only at nanometer scale (Bonijoly et al., 1982; Beyssac et al., 2003). Nevertheless, we speculate pressure should be also considered as a factor that can determine the degree of graphite crystallinity during both graphitization and graphite structural modifications.~~

~~We have investigated the effects of shear strain and pressure on graphite crystallinity during shear deformation with aseismic velocities, using a starting material with uniform properties (i.e. highly crystalline graphite powder). In contrast, Kuo et al. (2014) and Oohashi et al. (2011) simulated fault motions in synthetic and natural carbonaceous material with variable degree of maturity at the start of the experiments (ranging from amorphous carbonaceous material to crystalline graphite). Both studies reported graphitization of carbonaceous material due to localized frictional heating rather than structural disordering. These experiments reveal the impact of seismic velocities on graphite structural order and the fact their findings differ so markedly from ours highlights the complexity of graphite transformations in fault zones.~~

Our microstructural observations provide some indications of the deformation processes that affected graphite structural order. The shiny slickenlined surfaces are composed of very fine-grained material visible as slip-localized zone on SEM images (Fig. 4d). Nanoscale observations reveal graphite grains within it occasionally form stacked kink-band structures, (Fig. 5b, c). This zone, which we assume accommodated most of the induced deformation, is underlined by a less deformed zone composed of larger graphite grains in a finer matrix that in places has developed as an anastomosing fabric, typical of creeping gouges (Fig. 4d). In rare places at SEM scale brittely fractured grains also occur (Fig. 4f and 5d). The interpreted

structures suggest that brittle processes operated during shearing, and we conclude that these processes resulted in the structural disorder of graphite, manifested as changes in the Raman spectra. This interpretation is in agreement with the conditions of our experiments (i.e. shearing with aseismic velocities took place at room temperature conditions), that typically would not induce temperatures high enough for ~~crystal plastic~~ductile processes. Furthermore, the microstructures and the inferred processes are exactly the same as those observed by Nakamura et al. (2015) in the Hidaka metamorphic belt, Japan.

~~We have investigated the effects of shear strain and pressure on graphite crystallinity during shear deformation with aseismic velocities, using a starting material with uniform properties (i.e. highly crystalline graphite powder). In contrast, Kuo et al. (2014) and Oohashi et al. (2011) simulated fault motions in synthetic and natural carbonaceous material with variable degree of maturity at the start of the experiments (ranging from amorphous carbonaceous material to crystalline graphite). Both studies reported graphitization of carbonaceous material due to localized frictional heating rather than structural disordering. These experiments reveal the impact of seismic velocities on graphite structural order and the fact their findings differ so markedly from ours highlights the complexity of graphite transformations in fault zones.~~

However, crustal fault zones do not only accommodate brittle deformation. At higher temperatures and confining pressures, localised shearing can operate by crystal plastic mechanisms (White et al., 1980). We hypothesize that graphite ~~crystallinity~~ structural order could ~~also~~ be influenced by ~~plastic~~ ductile deformation, as was also suggested in previous studies by Large et al. (1994), Bustin et al. (1995), Barzoi et al. (2015). Furthermore, Kuo et al. (2014) and Oohashi et al. (2011) simulated fault motions in synthetic and natural carbonaceous material with variable degree of maturity at the start of the experiments (ranging from amorphous carbonaceous material to crystalline graphite). Both studies reported graphitization of carbonaceous material due to localized frictional heating rather than structural disordering. These experiments reveal the impact of seismic velocities on graphite structural order and the fact their findings differ so markedly from ours further highlights the complexity of graphite transformations in fault zones. ~~Investigating this hypothesis and identifying the exact effects of strain on graphite crystallinity during ductile deformation remain goals for future research.~~

4.3 Implications for graphite thermometry

The ~~crystallographic structure~~structural order of graphite measured by Raman spectroscopy has been applied as a thermometer that relies on progressive maturation of originally-organic carbonaceous material during diagenesis and metamorphism. Previous studies have focused on calibrating this thermometer. The current best calibration is described by the following equation T (°C) = -445 * R2 + 641 ± 50 (Beyssac et al. 2002) by inferring a linear correlation between R2 ratio and peak metamorphic temperatures. However, this thermometer disregards the effects of mechanical modifications ~~of~~ on

the ~~graphite~~ structure of graphite aggregates, which this study has identified as having a substantial influence on the ~~graphite crystallinity~~ R2 ratios in deformed ~~rocks~~ graphite gouges at sub-seismic velocities.

Our experiments demonstrate ~~a shear strain dependent~~an increase of the R2 ratio of initially highly crystalline graphite powder due to brittle deformation (Fig. 3a; Table 2). In natural analogues, the pre-shear graphite would yield temperatures up to 641 ± 50 ºC (~~S1~~S1), which is the upper limit of the calibrated thermometer (Beyssac et al. 2002). Whereas, the sheared samples would indicate peak metamorphic temperatures as low as 347 ± 50 ºC (~~estimated from the most strained samples; S1~~S1). Thus, we experimentally prove that in active tectonic settings graphite thermometers may underestimate the peak metamorphic temperatures by < 300 ºC. In cataclasites from the Alpine Fault zone, New Zealand (Kirilova et al., ~~in press~~2017) and fault zones of the Hidaka metamorphic belt, Japan (Nakamura, et al., 2015), the graphite thermometer yields temperature discrepancies of more than 100 ºC compared to temperature estimates derived both from the surrounding high-grade amphibolite facies mylonites and the lower grade equilibrium cataclastic phases (marked by chlorite alteration). Barzoi (2015) also described differences of ~ 150 ºC in graphite temperatures between strained and less strained low grade metamorphic rocks from Parang Mountains, South Carpathians.

We conclude that the existing graphite thermometer is unreliable in active tectonic settings. Furthermore, a calibration of this thermometer may be impossible to achieve because both structural disorder of graphite and graphitization (Oohashi et al., 2013) are likely to be encountered in fault zones.~~We conclude that shear strain calibration of the current graphite thermometer is needed, and we propose an appropriate adjustment based on our dataset. Fig. 3a illustrates good correlation between the average R2 and the bulk shear strain measured within a sample, which can be described by the following equation (1):~~

~~$F(x) = 0.14017 * x^{0.30713} + 0.15629$ with a correlation coefficient $R^2 = 0.95$ (1)~~

~~where x = bulk shear strain.~~

~~However~~

~~, a calibration of the existing graphite thermometer could be still insufficient to permit reliable temperature estimates in active tectonic settings because both aseismic and seismic sliding velocities are likely to be encountered in fault zones, resulting in structural disorder of graphite or graphitization (Oohashi et al., 2013) respectively. Furthermore, it can be challenging to estimate shear strain in natural samples, so a strain calibrated graphite thermometer may be impossible to use in deformed rocks.~~

5. Conclusions

We have experimentally demonstrated graphite structural disorder, manifested as changes in the Raman spectra, by performing shear deformation experiments at aseismic sliding velocities insufficient to generate appreciable frictional heat on graphite gouges composed of powdered highly-organized graphite. Microstructural data presented here reveal that this is a result of brittle processes. Our findings clearly compromise the validity of the calibrated graphite thermometer by showing it may significantly underestimate the peak metamorphic temperatures in active tectonic settings.

~~We have experimentally demonstrated that graphite crystallinity can be reduced by deformation by performing shear deformation experiments at aseismic sliding velocities insufficient to generate appreciable frictional heat on graphite gouges composed of powdered highly-organized graphite. Our results clearly demonstrate significant decrease in graphite structural order, which is a function of the total shear strain attained during the various experiments. Microstructural data presented here reveal that this is a result of brittle processes. We also observed a trend of increasing shear strain within a sample with increase in the applied normal stresses and sliding velocities. This reveals the complexity of graphite structural modifications and highlights the significance of the various parameters that can affect the graphitization process. Our findings compromise the validity of the calibrated graphite thermometer by showing they may underestimate the peak metamorphic temperatures in active tectonic settings. We further suggest a simple shear strain calibration of this thermometer.~~

Acknowledgments

The research was funded by the Department of Geology, University of Otago, New Zealand, and Rutherford Discovery Fellowship RDF-UOO0612 awarded to Virginia Toy. We also acknowledge the 'Tectonics and Structure of Zealandia' subcontract to the University of Otago by GNS Science (under contract C05X1702 to the New Zealand Ministry of Business, Innovation and Employment). We thank our colleagues Gemma Kerr and Brent Pooley for assistance in sample preparation, and Hamish Bowman for helping with data visualization. We also wish to express our gratitude to Laura Halliday for generously offering to perform grain size analysis on our samples at the Department of Geography, University of Otago, New Zealand. And last but not least, we thank Marco Scuderi for valuable discussions and assistance throughout the experimental procedures.

References

Barzoi, S. C.: Shear stress in the graphitization of carbonaceous matter during the low-grade metamorphism from the northern Parang Mountains (South Carpathians)—Implications to graphite geothermometry, International Journal of Coal Geology, 146, 179-187, 2015.

Beeler, N. M.: Laboratory-observed faulting in intrinsically and apparently weak materials: Strength, seismic coupling, dilatancy, and pore-fluid pressure, The Seismogenic Zone of Subduction Thrust Faults, pp.370-449, 2007.

Beyssac, O., Goffé, B., Chopin, C. and Rouzaud, J. N.: Raman spectra of carbonaceous material in metasediments: a new geothermometer, Journal of Metamorphic Geology 20.9: 859-871, 2002a.

Beyssac, O., Rouzaud, J. N., Goffé, B., Brunet, F., and Chopin, C.: Graphitization in a high-pressure, low-temperature metamorphic gradient: a Raman microspectroscopy and HRTEM study, Contributions to Mineralogy and Petrology, 143(1), 19-31, 2002b.

Beyssac, O., Brunet, F., Petitet, J. P., Goffé, B., and Rouzand, J. N.: Experimental study of the microtextural and structural transformations of carbonaceous materials under pressure and temperature, European Journal of Mineralogy, 15(6), 937-951, 2003.

Bonijoly, M., Oberlin, M. and Oberlin, A.: A possible mechanism for natural graphite formation, International Journal of Coal Geology, 1.4: 283-312, 1982.

Buseck, P. R. and Beyssac, O.: From organic matter to graphite: Graphitization, Elements, 10.6: 421-426, 2014.

Bustin, R. M., Ross, J. V., and Rouzaud, J. N.: Mechanisms of graphite formation from kerogen: experimental evidence, International Journal of Coal Geology, 28(1), 1-36, 1995.

Collettini, C., Di Stefano, G., Carpenter, B., Scarlato, P., Tesei, T., Mollo, S., Trippetta, F., Marone, C., Romeo, G. and Chiaraluce, L.: A novel and versatile apparatus for brittle rock deformation, International Journal of Rock Mechanics and Mining Sciences, 66, 114-123, 2014.

Crespo, E., Luque, F. J., Barrenechea, J. F., and Rodas, M.: Influence of grinding on graphite crystallinity from experimental and natural data: implications for graphite thermometry and sample preparation, Mineralogical Magazine, 70(6), 697-707, 2006.

Kirilova, M., Toy, V., Timms, N., Halfpenny, A., Menzies, C., Craw, D., Beyssac, O., Sutherland, R., Townend, J., Boulton, C., Carpenter, B., Cooper, A., Grieve, J., Little, T., Morales, L., Morgan, C., Mori, H., Sauer, K., Schleicher, A., Williams, J., Craw, L.: Textural changes of graphitic carbon by tectonic and hydrothermal processes in an active plate boundary fault zone, Alpine Fault, New Zealand. In Gessner, K., Blenkinsop, T.G., Sorjonen-Ward, P., (eds), Geological Society, London, Special Publication ~~453~~ 'Advances in the Characterization of Ore-Forming Systems from Geological, Geochemical and Geophysical data', 453 SP453-13, ~~in press~~2017.

Kuo, L. W., Li, H., Smith, S. A., Di Toro, G., Suppe, J., Song, S. R., and Si, J.: Gouge graphitization and dynamic fault weakening during the 2008 Mw 7.9 Wenchuan earthquake, Geology, 42(1), 47-50, 2014.

Large, D. J., Christy, A. G., and Fallick, A. E.: Poorly crystalline carbonaceous matter in high grade metasediments: implications for graphitisation and metamorphic fluid compositions, Contributions to Mineralogy and Petrology, 116(1-2), 108-116, 1994.

Manatschal, G.: Fluid-and reaction-assisted low-angle normal faulting: evidence from rift-related brittle fault rocks in the Alps (Err Nappe, eastern Switzerland), Journal of Structural Geology, 21(7), 777-793, 1999.

Moore, D. E., and Lockner, D. A.: Crystallographic controls on the frictional behavior of dry and water-saturated sheet structure minerals, Journal of Geophysical Research: Solid Earth, 109(B3), 2004.

Morrow, C. A., Moore, D. E., and Lockner, D. A.: The effect of mineral bond strength and adsorbed water on fault gouge frictional strength, Geophysical Research Letters, 27(6), 815-818, 2000.

Nakamura, Y., Oohashi, K., Toyoshima, T., Satish-Kumar, M., and Akai, J.: Strain-induced amorphization of graphite in fault zones of the Hidaka metamorphic belt, Hokkaido, Japan, Journal of Structural Geology, 72: 142 – 161, 2015.

~~Di Toro, G., Han, R., Hirose, T., De Paola, N., Nielsen, S., Mizoguchi, K., Ferri, F., Cocco, M. and Shimamoto, T.: Fault lubrication during earthquakes, Nature, 471(7339), p.494., 2011.~~

~~.~~Oohashi, K., Hiros, T. and Shimamoto, T.: Shear-induced graphitization of carbonaceous materials during seismic fault motion: experiments and possible implications for fault mechanics, Journal of Structural Geology, 33.6: 1122-1134, 2011.

Oohashi, K., Hirose, T. and Shimamoto, T.: The occurrence of graphite-bearing fault rocks in the Atotsugawa fault system, Japan: origins and implications for fault creep, Journal of Structural Geology 38: 39-50, 2012.

Oohashi, K., Hirose, T. and Shimamoto, T.: Graphite as a lubricating agent in fault zones: An insight from low-to high-velocity friction experiments on a mixed graphite-quartz gouge, Journal of Geophysical Research: Solid Earth, 118(5), pp.2067-2084, 2013.

Pimenta, M.A., Dresselhaus, G., Dresselhaus, M.S., Cancado, L.G., Jorio, A. and Saito, R.: Studying disorder in graphite-based systems by Raman spectroscopy, Physical Chemistry Chemical Physics, 9(11), pp.1276-1290, 2007.

Rietmeijer, F. J., and Mackinnon, I. D.: Poorly graphitized carbon as a new cosmothermometer for primitive extraterrestrial materials. Nature, 315(6022), 733-736, 1985.

Rutter, E.H., Hackston, A.J., Yeatman, E., Brodie, K.H., Mecklenburgh, J. and May, S.E.: Reduction of friction on geological faults by weak-phase smearing, Journal of Structural Geology, 51, pp.52-60, 2013.

Savage, R. H.: Graphite lubrication, Journal of Applied Physics 19.1: 1-10, 1948.

Toy, V.G., Niemeijer, A.R., Renard, F. Wirth, R., and Morales, L.: Striation and slickenline development on quartz fault surfaces at crustal conditions: ~~origin~~ Origin and effect on friction, Journal of Geophysical Research: Solid Earth, doi: 10.1002/2016JB013498, ~~in press~~2017.

Tuinstra, F. and Koenig, J.L.: Raman spectrum of graphite, The Journal of Chemical Physics, 53(3), pp.1126-1130, 1970.

White, S. H., Burrows, S. E., Carreras, J., Shaw, N. D., and Humphreys, F. J.: On mylonites in ductile shear zones, Journal of Structural Geology, 2(1-2), 175-187, 1980.

Wopenka, B., and Pasteris, J. D.: Structural characterization of kerogens to granulite-facies graphite: applicability of Raman microprobe spectroscopy, The American Mineralogist, 78(5-6), 533-557, 1993.

Zulauf, G., Kleinschmidt, G., and Oncken, O.: Brittle deformation and graphitic cataclasites in the pilot research well KTB-VB (Oberpfalz, FRG), Geological Society, London, Special Publications, 54(1), 97-103, 1990.

Table 1. Summary of the conditions at which experiments were carried out and results.

Table 2. Summary of the relationship between shear strain and average R2 within a sample. The conditions of each experiment are also given as follows: applied normal stress in MPa, sliding velocities in µm/s and sliding displacement in mm.

Figure 1. Plots of mechanical data (a) friction coefficient, µ vs. displacement (b)~~, (c), (d)~~ friction coefficient, µ vs. shear strain (c) layer thickness vs displacement.

Figure 2. Representative Raman spectra illustrating: (i) the most ~~crystalline~~ structurally ordered graphite (left column) within a sample; (ii) graphite with average ~~crystallinity~~ structural order per sample (middle column); and (iii) the most disordered graphite (right column) encountered in each sample. The R2 ratio for each spectrum is also noted in italic font.

Figure 3. Plot of the average R2 ratio per sample vs (a) the shear strain accumulated during each experiment (b) the total frictional work estimated for each experiment.

Figure 4. SEM images, obtained from the deformed graphite gouge during experiment 8 (normal stress at 25 MPa with 1 µm/s sliding velocity), show: (a) Slickenlines ornamenting the shear surface; (b), (c) A well-compacted layer of aligned graphite grains, which make up the shear surface. Bright patches due to a differential charging effect; (d) A less deformed zone with typical cataclastic fabric, underlying the shear surface; (e) Dilated cleavage planes in large graphite grains filled with smaller platy graphite grains oriented sub-perpendicular to the shear direction; (f) Fractured graphite grains.

Supplementary material ~~1~~ 1 (~~S1~~S1). Raman data from 20 spectra per sample together with calculated R2 ratio and average R2 value for each sample. The last column represents temperature estimated by the current best calibration of a Raman-based thermometer: T (ºC) = - 445 * R2 + 641 ± 50.

Experiment number	Normal stress (MPa)	Sliding velocity (µm/s)	Displacement (mm)	Peak friction coefficient (μ_{peak})	Steady state friction coefficient (μ_{ss})	Shear strain maximum
1	5	1	20	0.53	*0.22*	17.70
2	5	1	10	0.53	0.22	8.17
3	5	1	5	0.52	*not reached*	4.23
4	5	10	20	0.53	0.24	20.45
5	5	100	20	0.57	0.22	16.89
6	5	100	10	0.55	0.22	9.80
7	5	100	5	0.57	*not reached*	3.87
8	25	1	20	0.43	0.17	21.45
9	25	10	20	0.43	0.17	31.86
10	25	100	20	0.41	0.14	46.77

Table 1. Summary of the conditions at which experiments were carried out and results.

Sample	Experimental conditions	Shear strain	Average R2 (error estimate ± 0.05)	Total frictional work
Pre-shear graphite	N/A	N/A	0.173	
Exp. 2	5 MPa, 1 μm/s, 10 mm	8.17	0.438	17.71138.8689
Exp. 6	5 MPa, 100 μm/s, 10 mm	9.80	0.430	46.636917.7506
Exp. 5	5 MPa, 100 μm/s, 20 mm	16.89	0.454	157.931432.0578
Exp. 1	5 MPa, 1μm/s, 20 mm	17.70	0.506	165.474825.885
Exp. 4	5 MPa, 10 μm/s, 20 mm	20.45	0.517	180.834630.5943
Exp. 8	25 MPa, 1 μm/s, 20 mm	21.45	0.520	192.900796.6089
Exp. 9	25 MPa, 10 μm/s, 20 mm	31.86	0.580	283.772192.4834
Exp. 10	25 MPa, 100 μm/s, 20 mm	46.77	0.604	424.035687.703

Table 2. Summary of the relationship between shear strain, average R2, and total frictional work within a sample. The conditions of each experiment are also given as follows: applied normal stress in MPa, sliding velocities in μm/s and sliding displacement in mm.

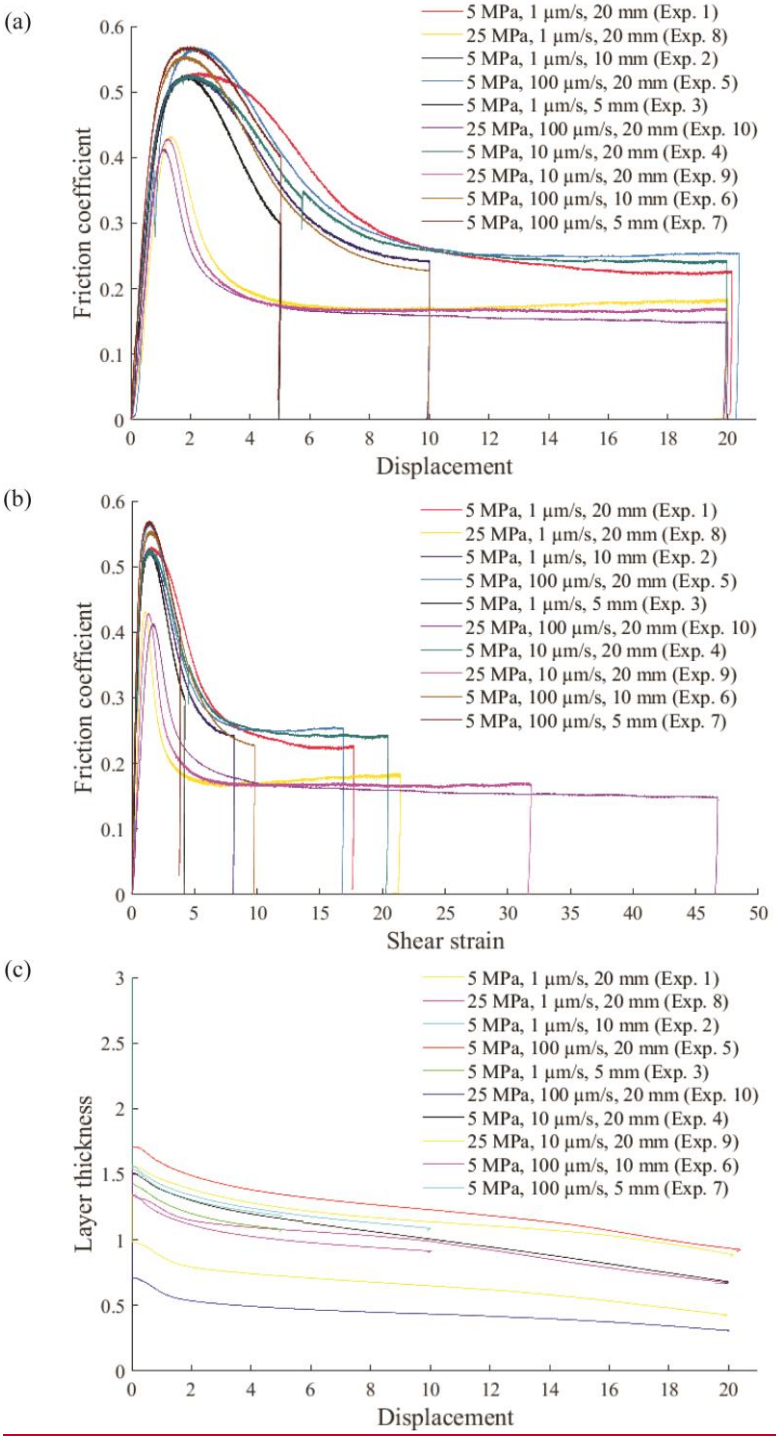

Figure 1. Plots of mechanical data (a) friction coefficient, µ vs. displacement (b) friction coefficient, µ vs. shear strain (c) layer thickness vs. displacement

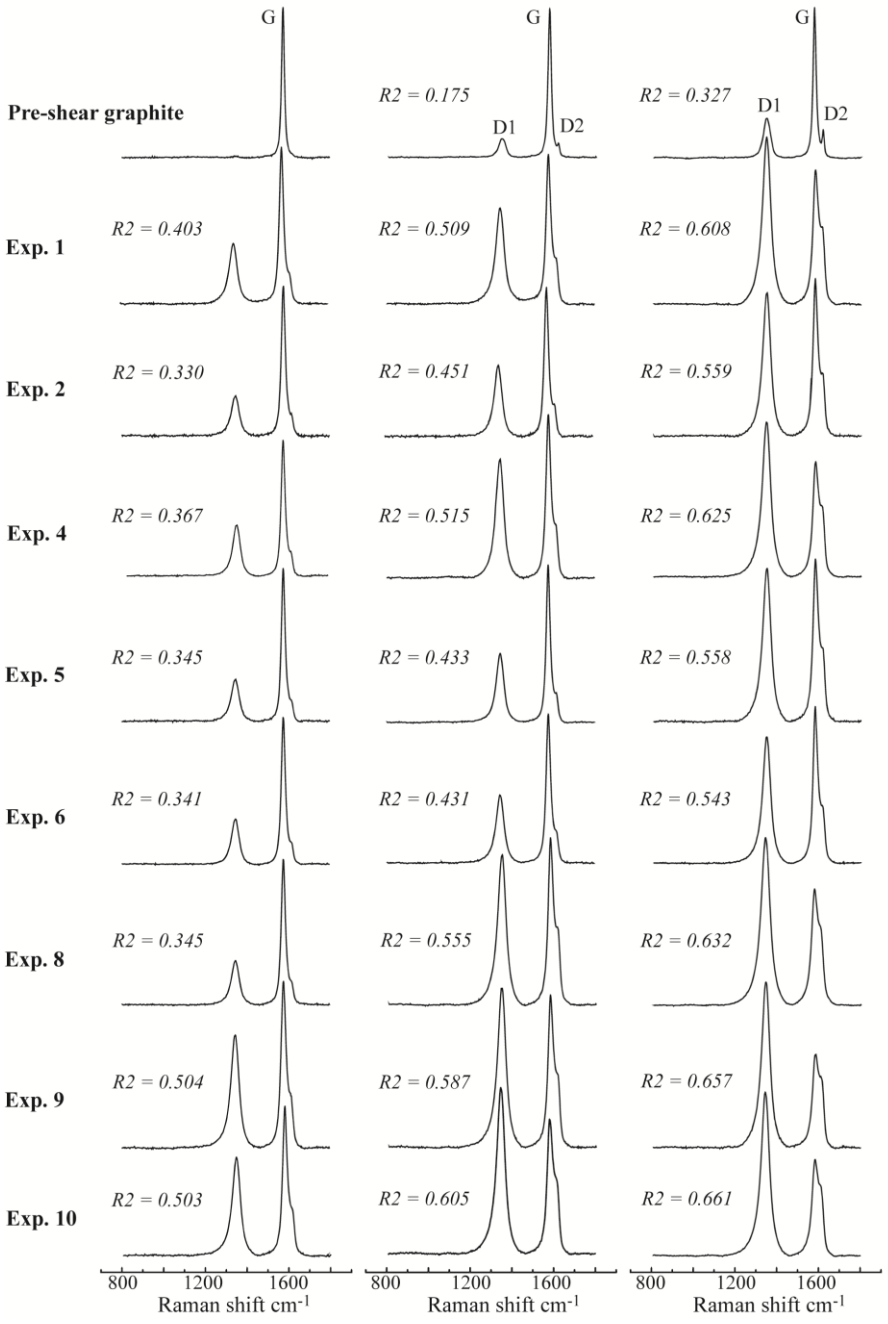

Figure 2. Representative Raman spectra illustrating: (i) the most crystalline graphite (left column) within a sample; (ii) graphite with average crystallinity per sample (middle column); and (iii) the most disordered graphite (right column) encountered in each sample. The R2 ratio (with an error estimate of 0.05) for each spectrum is also noted in italic font.

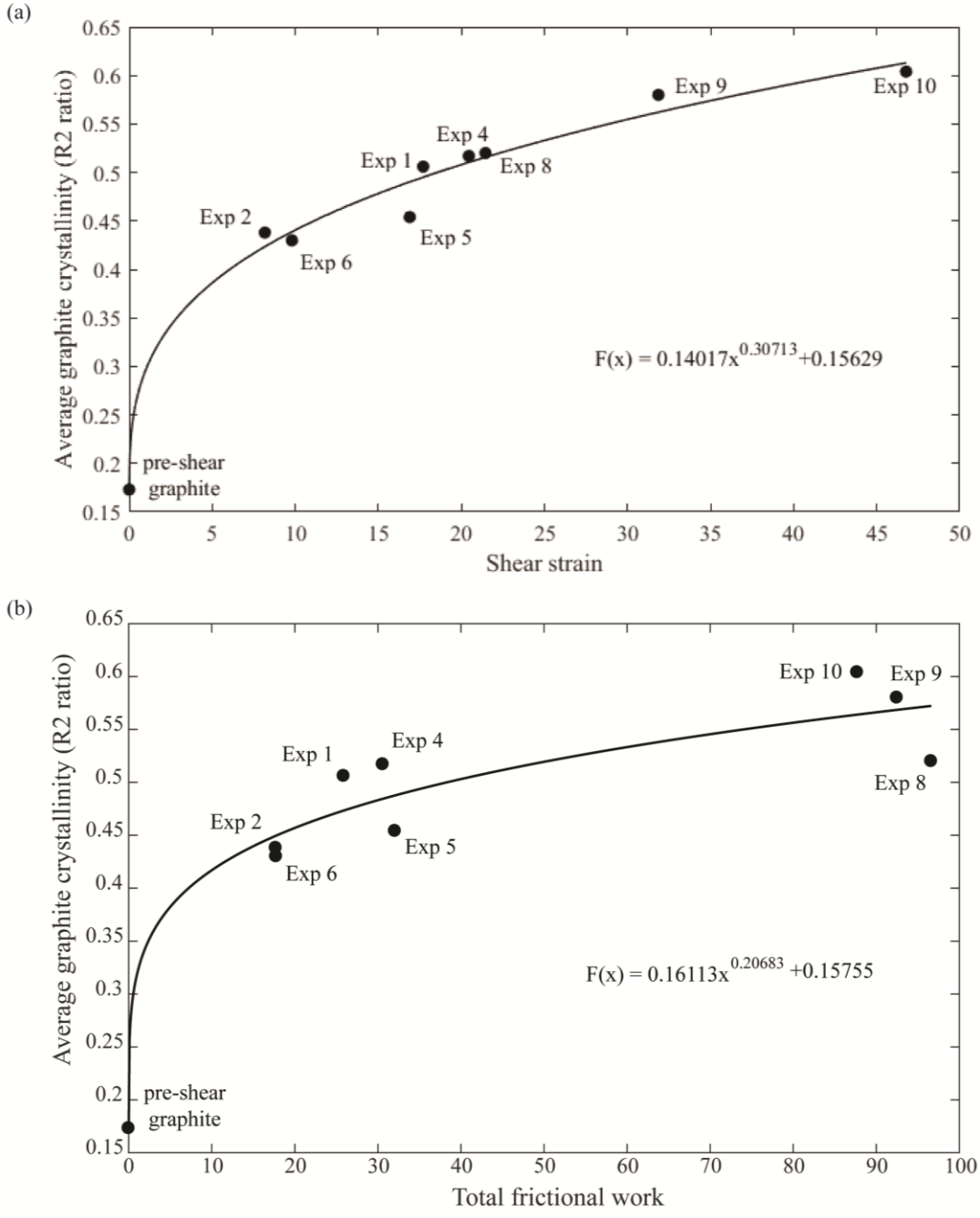

500

501 **Figure 3. (a)** Plot of the average R2 ratio vs. shear strain accumulated during each experiment. **(b)** Plot of the average R2
502 ratio vs. total frictional work during each experiment.

503

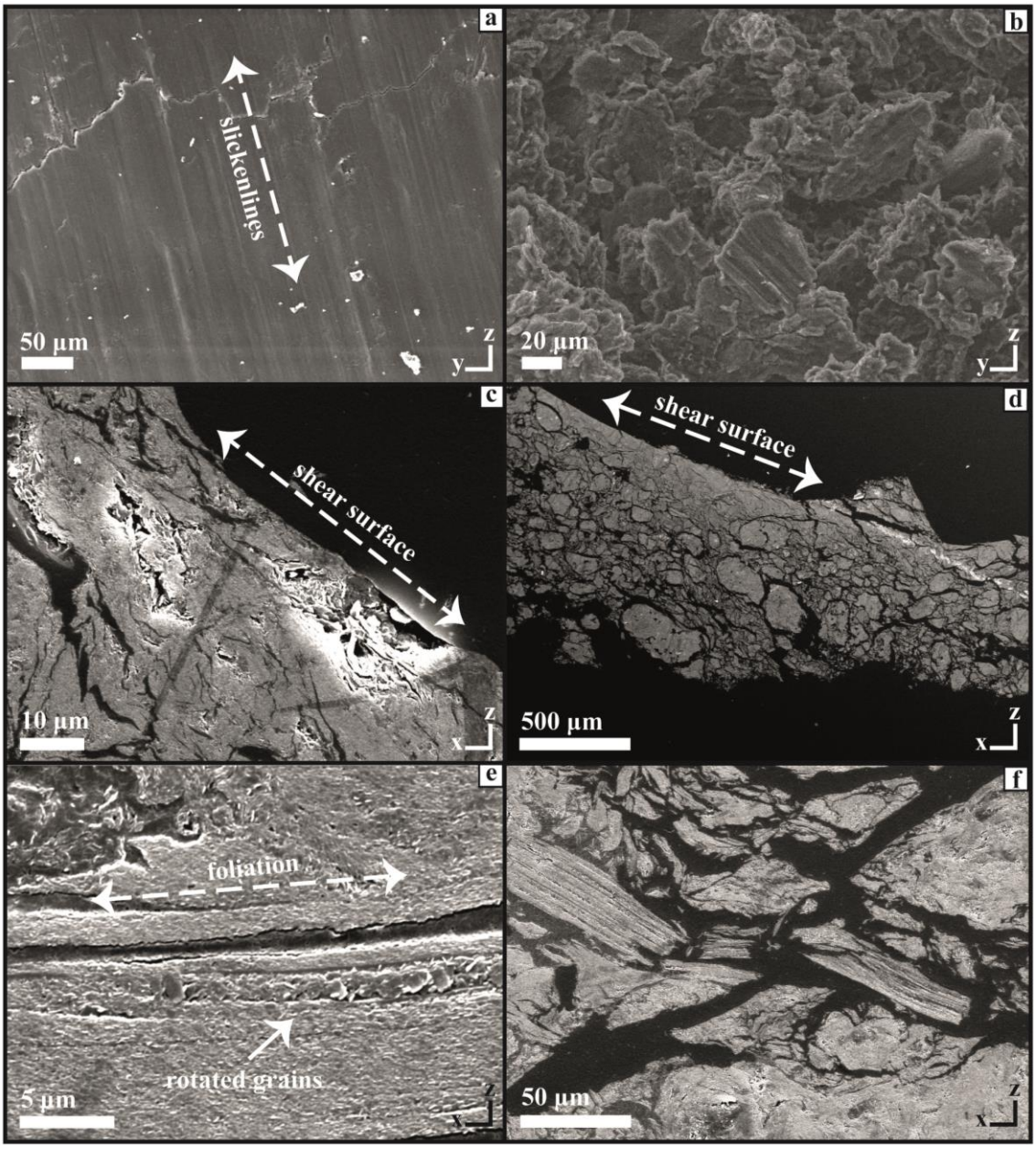

504

505 **Figure 4.** SEM images, obtained from the deformed graphite gouge during experiment 8 (normal stress at 25 MPa with 1
506 µm/s sliding velocity), show: (a) Slickenlines ornamenting the shear surface; (b), (c) A well-compacted layer of aligned
507 graphite grains, which make up the shear surface. Bright patches due to a differential charging effect; (d) A less deformed
508 zone with typical cataclastic fabric, underlying the shear surface; (e) Dilated cleavage planes in large graphite grains filled
509 with smaller platy graphite grains oriented sub-perpendicular to the shear direction; (f) Fractured graphite grains.

510

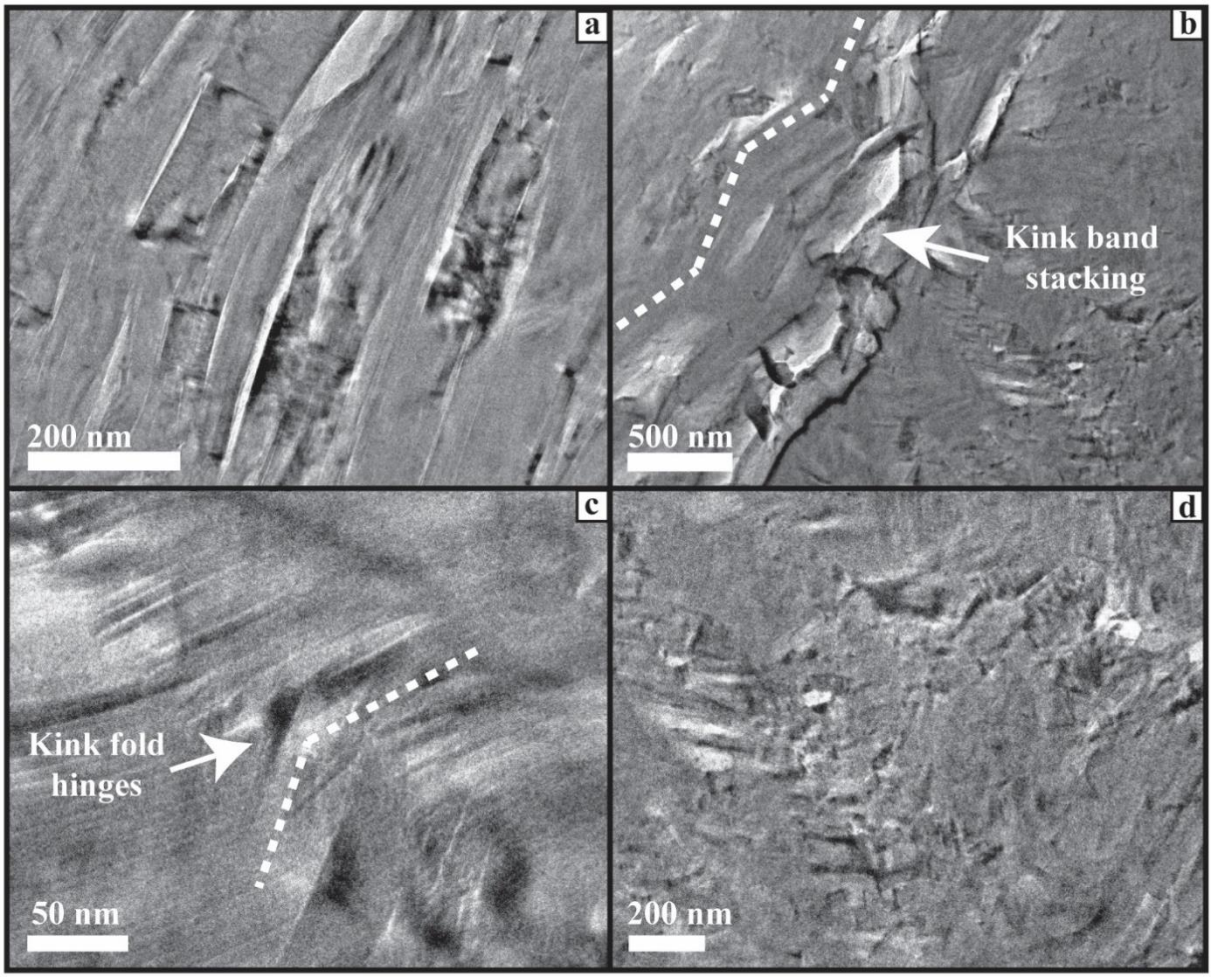

Figure 5 TEM images showing microstructural characteristics of the slip-localized shear surface: (a) aligned grains showing slightly different orientation; (b) kink band stacking; (c) dilated kink fold hinges; (d) fragmented grains.